Supplemental file 1, related to MATERIALS AND METHODS. Plasmids and Yeast Strains Used in This Study

Plasmids for *Saccharomyces cerevisiae* Expression

Plasmid	Mutations	Reference
pRS416	N/A	(Sikorski and Hieter, 1989)
pRS414	N/A	(Sikorski and Hieter, 1989)
pRS416-*SNF7*	Wild-type	(Henne et al., 2012)
pRS414-*SNF7*	Wild-type	this study
pRS416-*snf7*^{Q90C}	Q90C	this study
pRS416-*snf7*^{M130C}	M130C	this study
pRS416-*snf7*$^{Q90C\ M130C}$	Q90C M130C	this study
pRS416-*snf7*^{T20C}	T20C	this study
pRS416-*snf7*^{K35C}	K35C	this study
pRS416-*snf7*^{K60C}	K60C	this study
pRS416-*snf7*^{E88C}	E88C	this study
pRS416-*snf7*^{H118C}	H118C	this study
pRS416-*snf7*^{G140C}	G140C	this study
pRS416-*snf7*$^{E88C\ H118C}$	E88C H118C	this study
pRS416-*snf7*$^{K60C\ A66C}$	K60C A66C	this study
pRS416-*snf7*^{T83E}	T83E	this study
pRS416-*snf7*^{M87E}	M87E	this study
pRS416-*snf7*^{Q90K}	Q90K	this study
pRS416-*snf7*^{I94E}	I94E	this study
pRS416-*snf7*^{A97K}	A97K	this study
pRS416-*snf7*^{L99K}	L99K	this study
pRS416-*snf7*^{L101E}	L101E	this study
pRS416-*snf7*^{T103E}	T103E	this study
pRS416-*snf7*^{M104E}	M104E	this study
pRS416-*snf7*^{M107E}	M107E	this study
pRS416-*snf7*^{M114E}	M114E	this study
pRS416-*snf7*^{I117E}	I117E	this study
pRS416-snf7^{L121D}	L121D	(Saksena et al., 2009)
pRS416-*snf7*^{R25E}	R25E	this study
pRS416-*snf7*^{H29E}	H29E	this study
pRS416-*snf7*^{K36E}	K36E	this study
pRS416-*snf7*^{E95K}	E95K	this study
pRS416-*snf7*^{E102K}	E102K	this study
pRS416-*snf7*^{E109K}	E109K	this study
pRS414-*snf7*$^{R25E\ K36E}$	R25E K36E	this study
pRS416-*snf7*$^{E95K\ E109K}$	E95K E109K	this study
pRS414-*snf7*$^{R25E\ H29E\ K36E}$	R25E H29E K36E	this study
pRS416-*snf7*$^{E95K\ E102K\ E109K}$	E95K E102K E109K	this study

pRS414-*snf7*^{K35C}	K35C	this study
pRS416-*snf7*^{A63C}	A63C	this study
pRS416-*snf7*^{K69C}	K69C	this study
pRS416-*snf7*^{Q75C}	Q75C	this study
pRS416-*snf7*^{E81C}	E81C	this study
pRS416-*snf7*^{E95C}	E95C	this study
pRS416-*snf7*^{E102C}	E102C	this study
pRS416-*snf7*^{V126E}	V126E	this study
pRS416-*snf7*^{M130E}	M130E	this study
pRS416-*snf7*^{I133E}	I133E	this study
pRS416-*snf7*^{A51E}	A51E	this study
pRS416-*snf7*^{L55E}	L55E	this study
pRS416-*snf7*^{L67E}	L67E	(Henne et al., 2012)
pRS416-*snf7*^{N59P}	N59P	this study
pRS416-*snf7*^{E102P}	E102P	this study
pRS416-*snf7*^{L121P}	L121P	this study

Plasmids for *Escherichia coli* Expression for Protein Purification

Plasmid	Mutations	Reference
pET28a-*SMT3-snf7*$^{12-150}$	*SMT3-snf7*N12-P150	this study
pET23d-*snf7*^{R52E}	R52E	(Henne et al., 2012)
pET23d-*snf7*$^{R52E\ E88C\ H118C}$	R52E E88C H118C	this study
pET23d-*snf7*$^{R52E\ E88C\ G140C}$	R52E E88C G140C	this study
pET23d-*snf7*$^{R52E\ H118C\ G140C}$	R52E H118C G140C	this study
pET23d-*snf7*$^{R52E\ T20C}$	R52E T20C	this study
pET23d-*snf7*$^{R52E\ K35C}$	R52E K35C	this study
pET23d-*snf7*$^{R52E\ K60C}$	R52E K60C	this study
pET23d-*snf7*$^{R52E\ E88C}$	R52E E88C	this study
pET23d-*snf7*$^{R52E\ H118C}$	R52E H118C	this study
pET23d-*snf7*$^{R52E\ G140C}$	R52E G140C	this study
pET23d-*snf7*$^{R52E\ K60C\ A66C}$	R52E K60C A66C	this study
pET23d-*snf7*$^{R52E\ Q90K}$	R52E Q90K	this study
pET23d-*snf7*$^{R52E\ I94E}$	R52E I94E	this study
pET23d-*snf7*$^{R52E\ M107E}$	R52E M107E	this study
pET23d-*snf7*$^{R52E\ M114E}$	R52E M114E	this study
pET23d-*snf7*$^{R52E\ R25E\ H29E\ K36E}$	R52E R25E H29E K36E	this study
pET23d-*snf7*$^{R52E\ E95K\ E102K\ E109K}$	R52E E95K E102K E109K	this study
pET23d-*snf7*$^{R52E\ V126E}$	R52E V126E	this study
pET23d-*snf7*$^{R52E\ I133E}$	R52E I133E	this study
pET23d-*VPS24*	Wild-type	(Henne et al., 2012)
pET23d-*VPS2*	Wild-type	(Henne et al., 2012)

Yeast Strains Used in This Study		
Strain	**Genotype**	**Reference**
SEY6210.1	*Mat a, leu2-3, 2-112, ura3-52, his3-Δ200, trp1-Δ901, lys2-801, suc2-Δ9*	(Robinson et al., 1988)
MBY24	SEY6210.1; *snf7Δ::HIS3*	(Babst et al., 2002)
NBY44	SEY6210.1; *snf7Δ::HIS3; MUP1-PHLOURIN::KAN*	(Henne et al., 2012)

eLIFE elifesciences.org

RESEARCH ARTICLE

Figures and figure supplements

Structural basis for activation, assembly and membrane binding of ESCRT-III Snf7 filaments

Shaogeng Tang *et al*

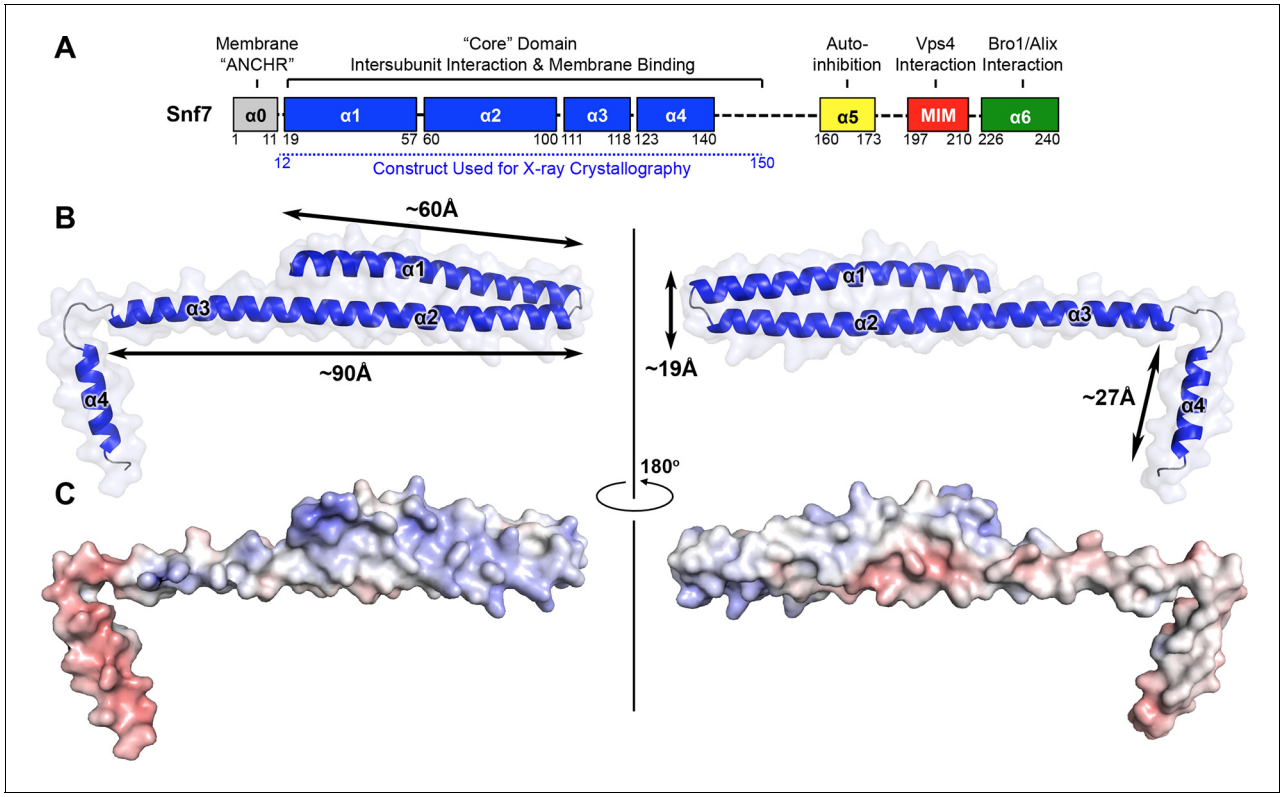

Figure 1. X-ray Crystal Structure of Snf7^{core} (**A**) The domain organization of Snf7. The core domain used for X-ray crystallography is shown in blue. (**B**) Overlay of ribbon and space-filling models of the X-ray crystal structure of Snf7^{core}. (**C**) Electrostatic surface potential of Snf7^{core} with positively charged regions in blue (+10kcal/e$^-$) and negatively charged regions in red (-10kcal/e$^-$). See also ***Table 1***.

DOI: http://dx.doi.org/10.7554/eLife.12548.003

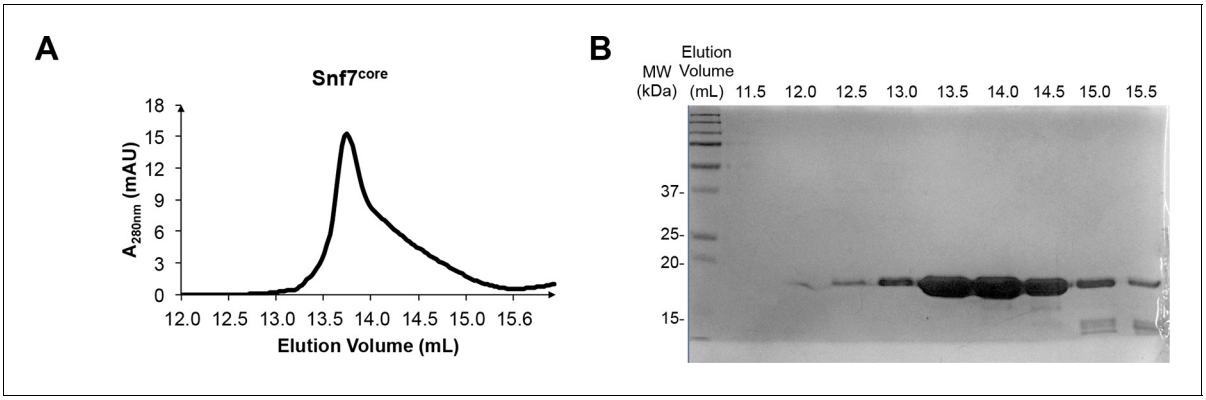

Figure 1—figure supplement 1. Protein purification of Snf7^{core} (**A**) A superdex-200 gel filtration size exclusion chromatogram of Snf7^{core}. (**B**) A SDS-PAGE Coomassie brilliant blue staining of the gel filtration fractions corresponding to Snf7^{core}.

DOI: http://dx.doi.org/10.7554/eLife.12548.004

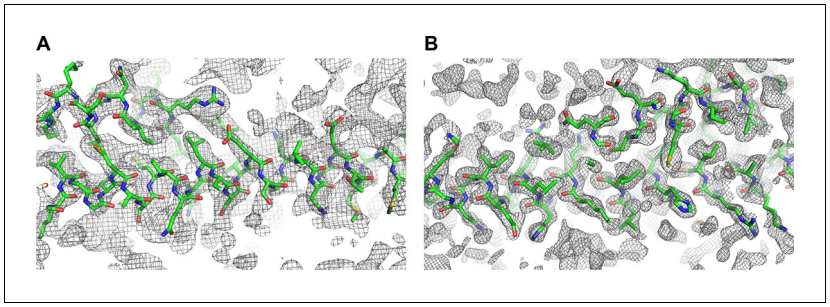

Figure 1—figure supplement 2. 2Fc-Fo simulated-annealing composite-omit electron density maps contoured at 1.0σ of Snf7^{core} open conformations (**A**) A and (**B**) B.
DOI: http://dx.doi.org/10.7554/eLife.12548.005

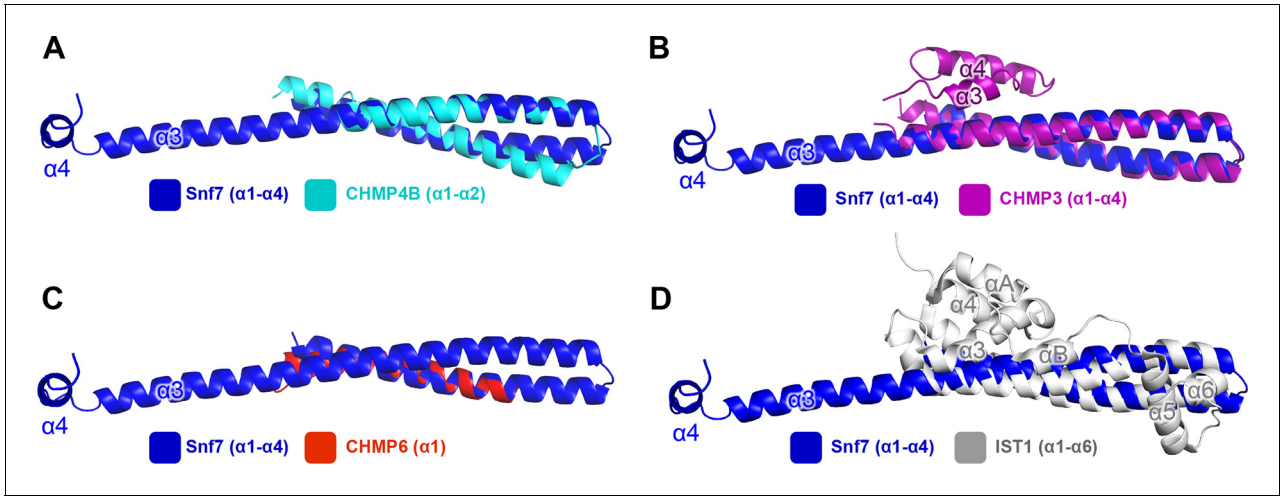

Figure 1—figure supplement 3. Superimposing Snf7^{core} (blue) with (**A**) CHMP4B$^{\alpha1\text{-}\alpha2}$ (cyan) (PDB: 4ABM), with (**B**) CHMP3$^{\alpha1\text{-}\alpha4}$ (purple) (PDB: 3FRT), with (**C**) CHMP6$^{\alpha1}$ (red) (PDB: 3HTU) Snf7^{core}, and with (**D**) IST1$^{\alpha1\text{-}\alpha6}$ (grey) (PDB: 3FRR).

DOI: http://dx.doi.org/10.7554/eLife.12548.006

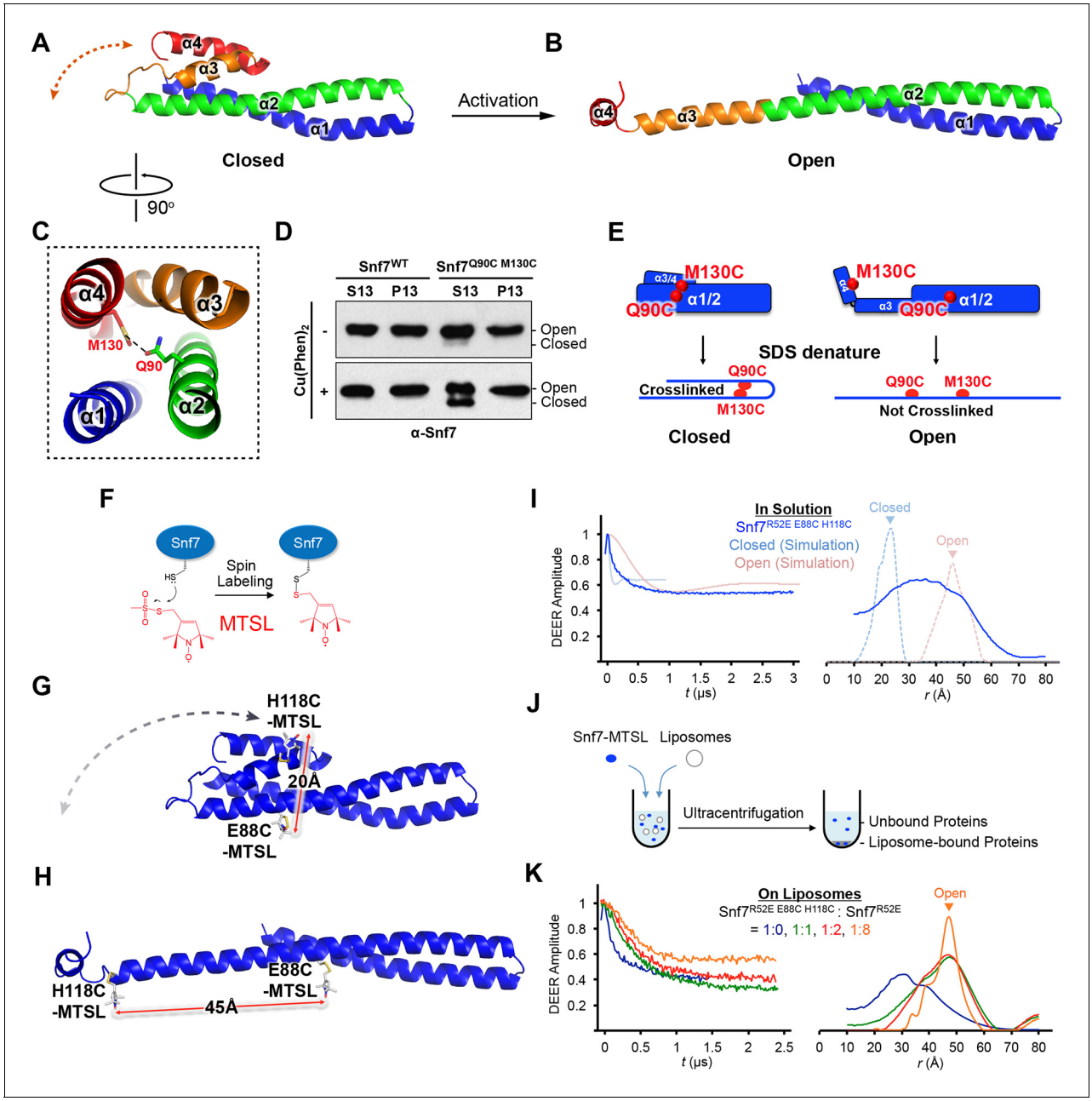

Figure 2. Conformational Rearrangement of Snf7 (**A–B**) Ribbon diagrams of (**A**) a homology model of closed Snf7^{core} (***Henne et al., 2012***) and (**B**) the X-ray crystal structure of open Snf7^{core}. (**C**) A close-up view of the side chain interaction between Gln90 and Met130. (**D**) Western blotting and subcellular fractionation of *snf7*Δ yeast exogenously expressing *SNF7* or *snf7*$^{Q90C\ M130C}$with and without copper(II) 1,10-phenanthroline. (**E**) Schematic showing closed and open Snf7^{core} with cysteines (red dots) before and after SDS-denaturing. (**F**) Snf7 site-directed spin-labeling with MTSL (red). (**G–H**) Distance between Glu88 and His118 of (**G**) closed and (**H**) open Snf7 shown in ribbon. (**I** and **K**) Time domain signals and distance distributions from DEER spectroscopy of (**I**) Snf7$^{R52E\ E88C\ H118C}$ in solution, and simulated closed and open Snf7$^{core\ E88C\ H118C}$ using *MMM*, and (**K**) Snf7$^{R52E\ E88C\ H118C}$: Snf7^{R52E} (1:0, 1:1, 1:2, and 1:8) with liposomes. (**J**) Schematic showing liposome sedimentation for DEER. MTSL-labeled Snf7 proteins (blue oval) and liposomes (grey circle).

DOI: http://dx.doi.org/10.7554/eLife.12548.008

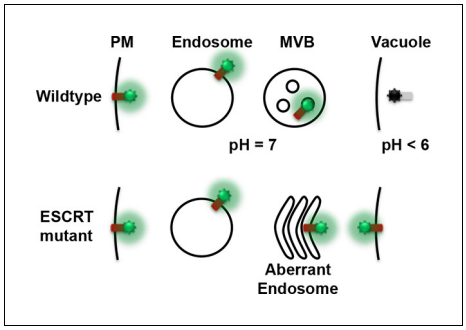

Figure 2—figure supplement 1. Conceptual model for the Mup1-pHluorin MVB sorting assay.
DOI: http://dx.doi.org/10.7554/eLife.12548.009

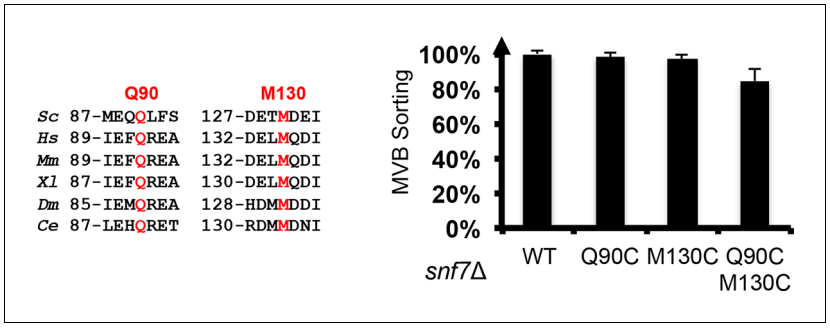

Figure 2—figure supplement 2. Sequence alignments of Snf7 α2 and α4, with conserved Gln90 and Met130 shown in red, and quantitative MVB sorting data for *snf7*Δ yeast exogenously expressing *SNF7*, $snf7^{Q90C}$, $snf7^{M130C}$, and $snf7^{Q90C\ M130C}$. Error bars represent standard deviations.

DOI: http://dx.doi.org/10.7554/eLife.12548.010

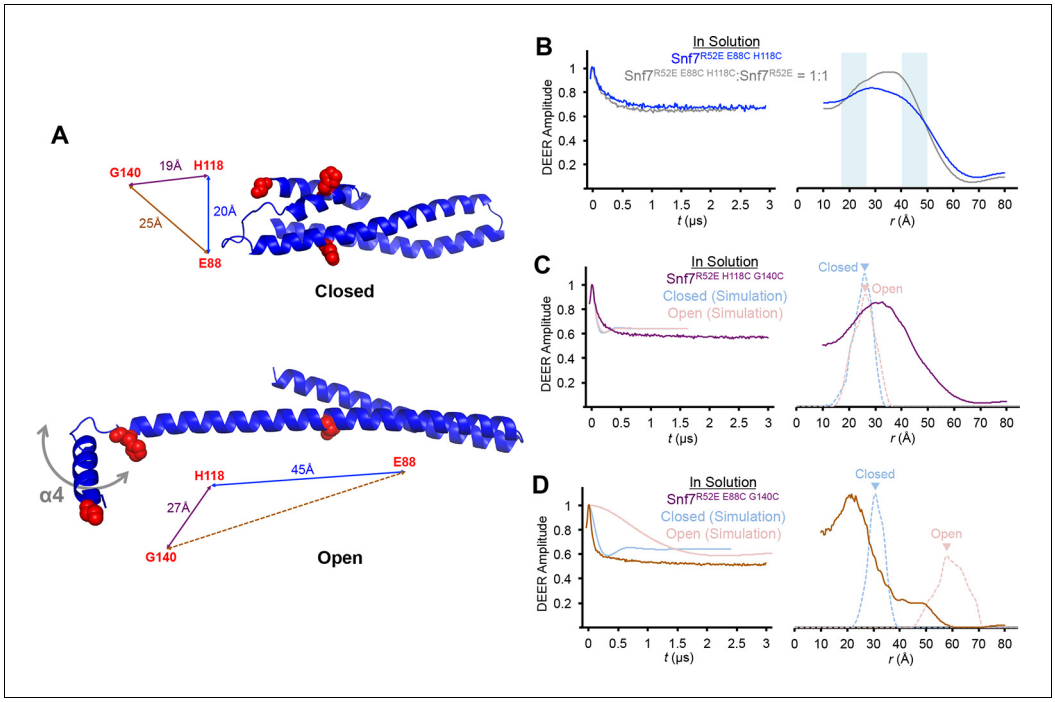

Figure 2—figure supplement 3. Time domain signals and distance distributions from DEER spectroscopy of full-length Snf7$^{R52E\ E88C\ H118C}$, Snf7$^{R52E\ H118C\ G140C}$ and Snf7$^{R52E\ E88C\ G140C}$. (**A**) Ribbon models of closed and open Snf7^{core} showing inter-residue distances between E88, H118 and G140. (**B–D**) Time domain signals and distance distributions from DEER spectroscopy of (**B**) full-length Snf7$^{R52E\ E88C\ H118C}$, and full-length Snf7$^{R52E\ E88C\ H118C}$:Snf7^{R52E} (1:1) in solution, (**C**) full-length Snf7$^{R52E\ H118C\ G140C}$in solution and simulated closed and open Snf7$^{core\ H118C\ G140C}$ using *MMM*, and (**D**) full-length Snf7$^{R52E\ E88C\ G140C}$ in solution and simulated closed and open Snf7$^{core\ E88C\ G140C}$ using *MMM*. Blue shaded portions of the distributions indicate distance ranges that can be attributed to open and closed conformations.

DOI: http://dx.doi.org/10.7554/eLife.12548.011

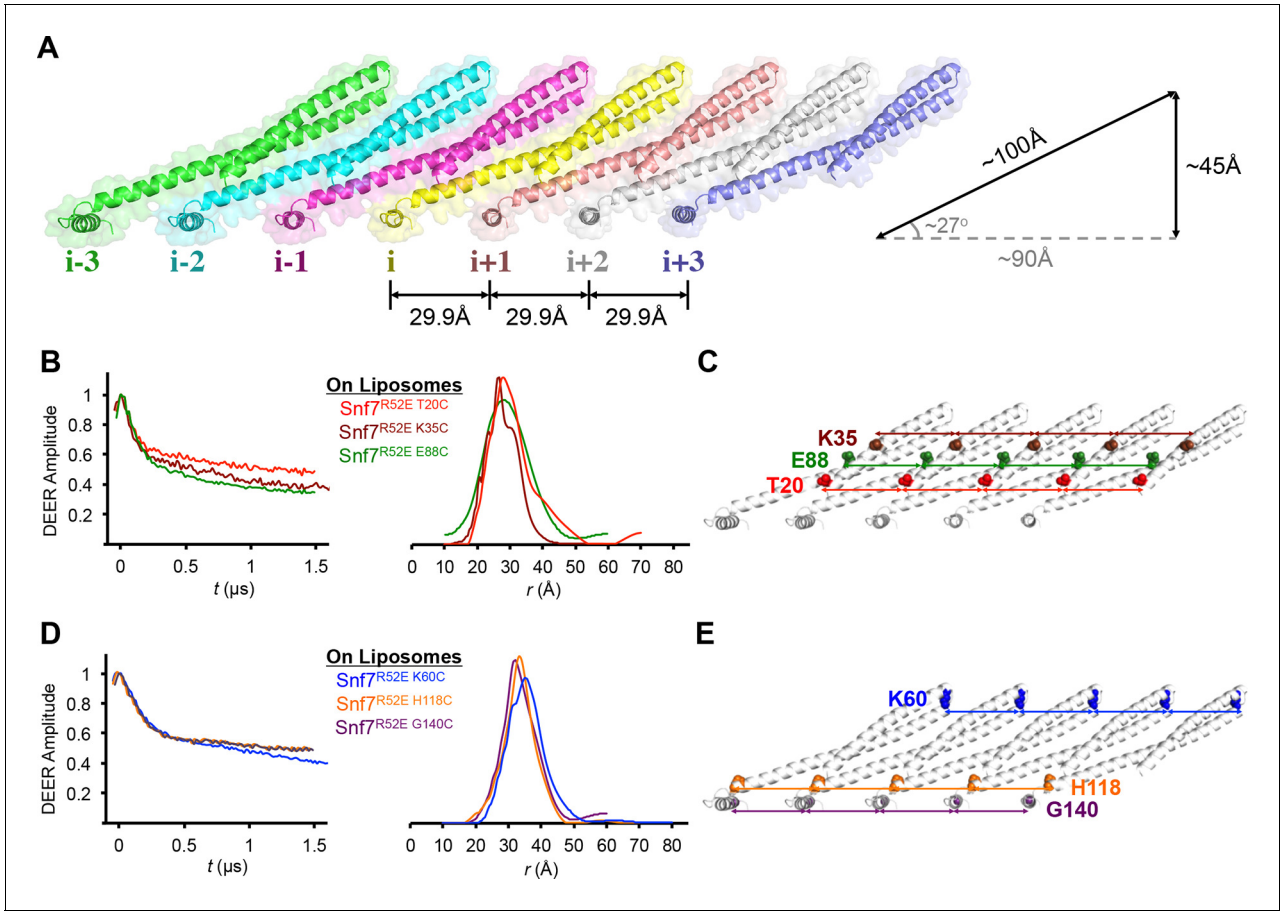

Figure 3. Membrane-bound Snf7 Protofilament with ~30 Å Periodicity (**A**) Overlay of ribbon and space-filling models of a 7-mer Snf7 protofilament with measured dimensions. (**B** and **D**) Time domain signals and distance distributions from DEER spectroscopy of (**B**) full-length $Snf7^{R52E\ T20C}$, $Snf7^{R52E\ K35C}$, and $Snf7^{R52E\ E88C}$ with liposomes, (**D**) full-length $Snf7^{R52E\ K60C}$, $Snf7^{R52E\ H118C}$, and $Snf7^{R52E\ G140C}$ with liposomes. (**C** and **E**) Schematic showing the spin label positions in a Snf7 protofilament.

DOI: http://dx.doi.org/10.7554/eLife.12548.012

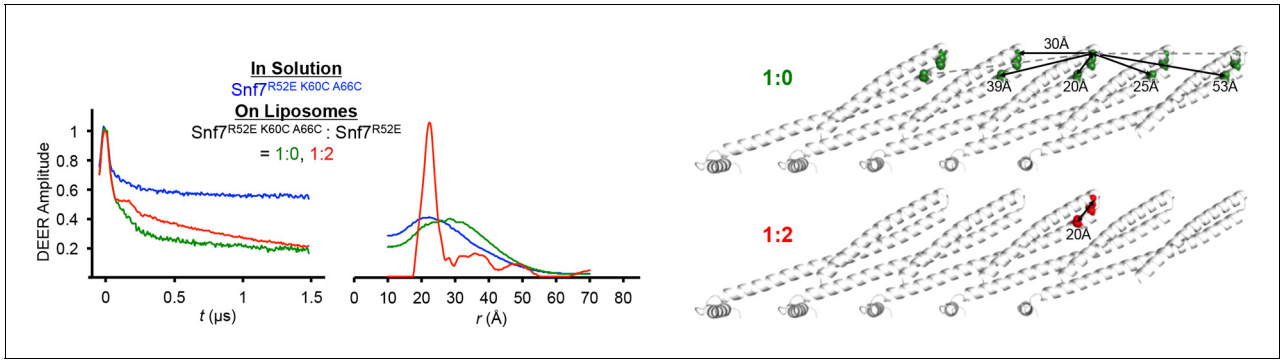

Figure 3—figure supplement 1. Time domain signals and distance distributions from DEER spectroscopy of full-length Snf7$^{R52E\ K60C\ A66C}$ in solution and full-length Snf7$^{R52E\ K60C\ A66C}$: Snf7^{R52E} (1:0, 1:2) with liposomes, and schematic showing the locations of the spin label positions in a Snf7 protofilament.
DOI: http://dx.doi.org/10.7554/eLife.12548.013

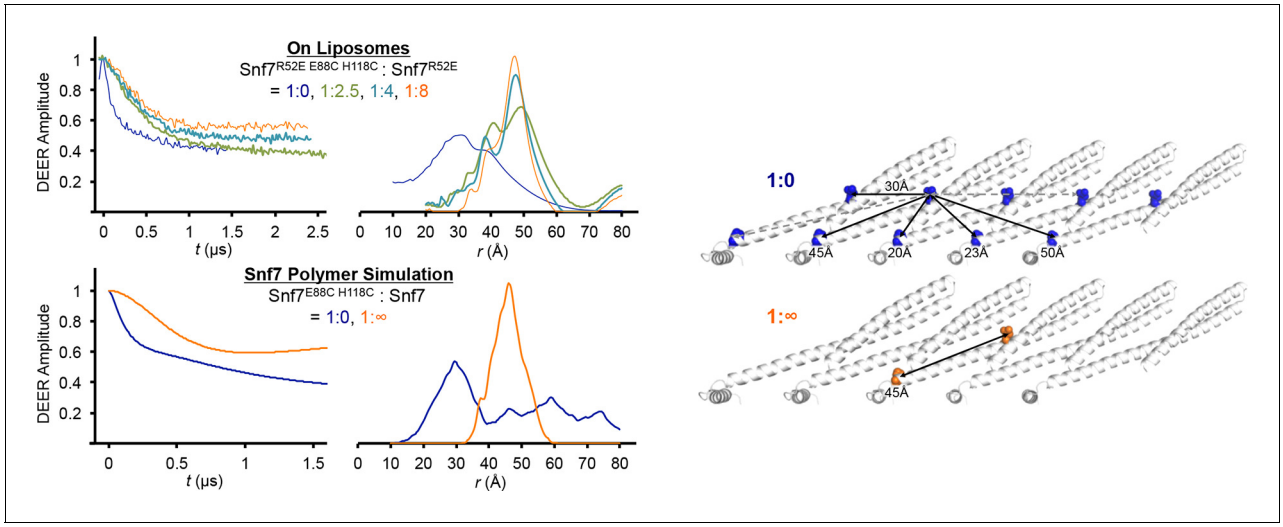

Figure 3—figure supplement 2. Time domain signals and distance distributions from DEER spectroscopy of full-length Snf7$^{R52E\ E88C\ H118C}$: Snf7^{R52E} (1:0, 1:2.5, 1:4, 1:8) with liposomes and simulated Snf7$^{core\ E88C\ H118C}$: Snf7^{core} (1:0, 1: ∞) polymers using *MMM*, and schematic showing the locations of the spin label positions in a Snf7 protofilament. The full-length Snf7$^{R52E\ E88C\ H118C}$: Snf7^{R52E} (1:0 and 1:8) with liposomes datasets are re-plotted from ***Figure 2K*** as shown in fine lines.

DOI: http://dx.doi.org/10.7554/eLife.12548.014

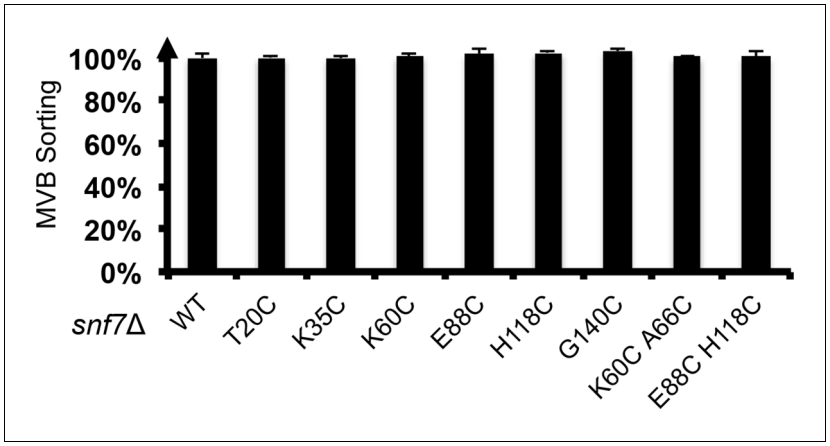

Figure 3—figure supplement 3. Quantitative MVB sorting data for *snf7*Δ yeast exogenously expressing *SNF7*, $snf7^{T20C}$, $snf7^{K35C}$, $snf7^{K60C}$, $snf7^{E88C}$, $snf7^{H118C}$, $snf7^{G140C}$, $snf7^{K60C\ A66C}$ and $snf7^{E88C\ H118C}$. Error bars represent standard deviations.

DOI: http://dx.doi.org/10.7554/eLife.12548.015

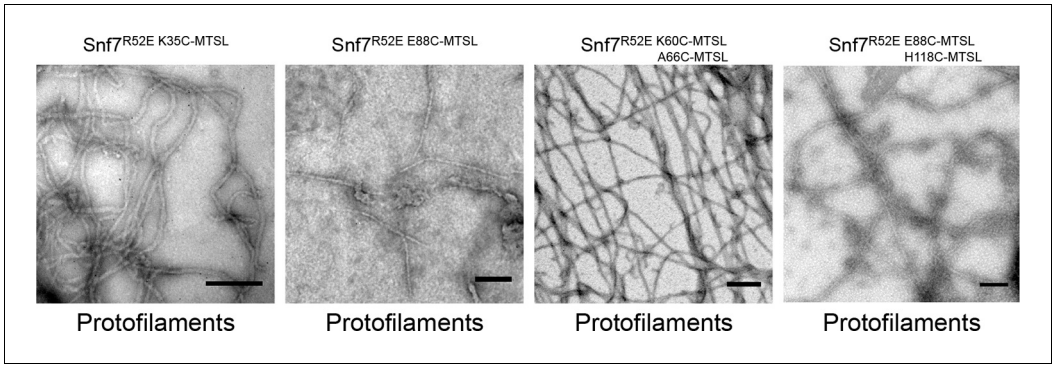

Figure 3—figure supplement 4. Representative TEM images of recombinant full-length $Snf7^{R52E\ K35C}$, $Snf7^{R52E\ E88C}$, $Snf7^{R52E\ K60C\ A66C}$, and $Snf7^{R52E\ E88C\ H118C}$ labeled with MTSL. Scale bars, 200 nm.

DOI: http://dx.doi.org/10.7554/eLife.12548.016

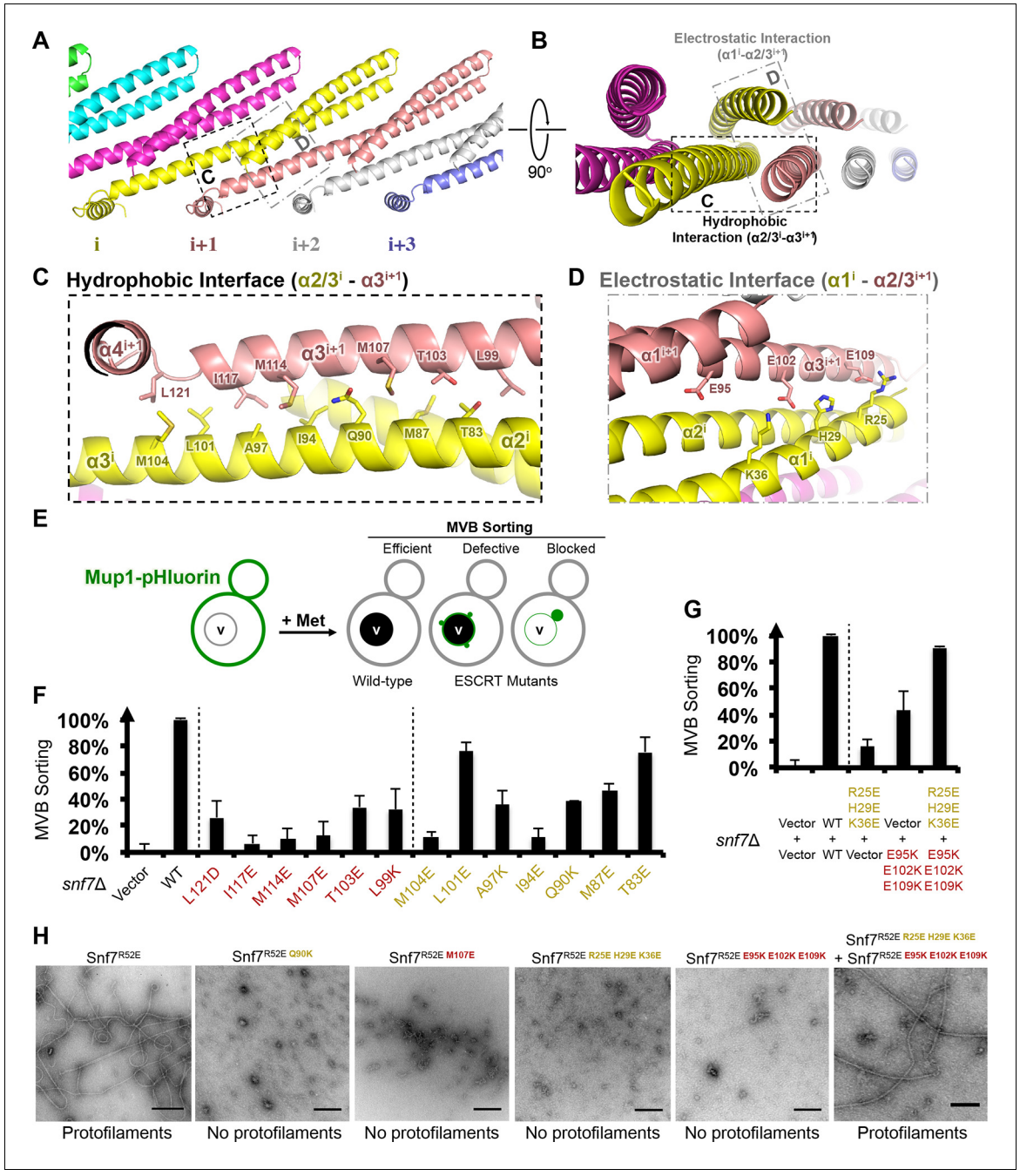

Figure 4. Hydrophobic and Electrostatic Interactions in a Snf7 Filament (**A–B**) Ribbon models of a Snf7 protofilament. The hydrophobic protein interface is shown in black dash-line and the electrostatic interface in grey dash-dot line. (**C–D**) Close-up views of the hydrophobic interface between $\alpha2/3^{i}$ and $\alpha3^{i+1}$ and the electrostatic interface between $\alpha1^{i}$ and $\alpha2/3^{i+1}$. Protomer (**i**) shown in yellow and protomer (i+1) in red. (**E**) Conceptual model for the Mup1-pHluorin MVB sorting assay. Vacuole (**v**). (**F**) Quantitative MVB sorting data for *snf7*Δ yeast exogenously expressing empty vector, *SNF7*, $snf7^{L121D}$, $snf7^{I117E}$, $snf7^{M114E}$, $snf7^{M107E}$, $snf7^{T103E}$, $snf7^{L99K}$, $snf7^{M104E}$, $snf7^{L101E}$, $snf7^{A97K}$, $snf7^{I94E}$, $snf7^{Q90K}$, $snf7^{M87E}$, and $snf7^{T83E}$. Error bars represent standard deviations. (**G**) Quantitative MVB sorting data for *snf7*Δ yeast exogenously expressing empty vectors, *SNF7*, $snf7^{R25E\ H29E\ K36E}$and empty vector, empty vector and $snf7^{E95K\ E102K\ E109K}$, and $snf7^{R25E\ H29E\ K36E}$ and $snf7^{E95K\ E102K\ E109K}$. Error bars represent standard deviations. (**H**) Representative TEM images of recombinant full-length $Snf7^{R52E}$, $Snf7^{R52E\ Q90K}$, $Snf7^{R52E\ M107E}$, $Snf7^{R52E\ R25E\ H29E\ K36E}$, $Snf7^{R52E\ E95K\ E102K\ E109K}$, and $Snf7^{R52E\ R25E\ H29E\ K36E}$ and $Snf7^{R52E\ E95K\ E102K\ E109K}$ (1:1). Scale bars, 200 nm.

DOI: http://dx.doi.org/10.7554/eLife.12548.017

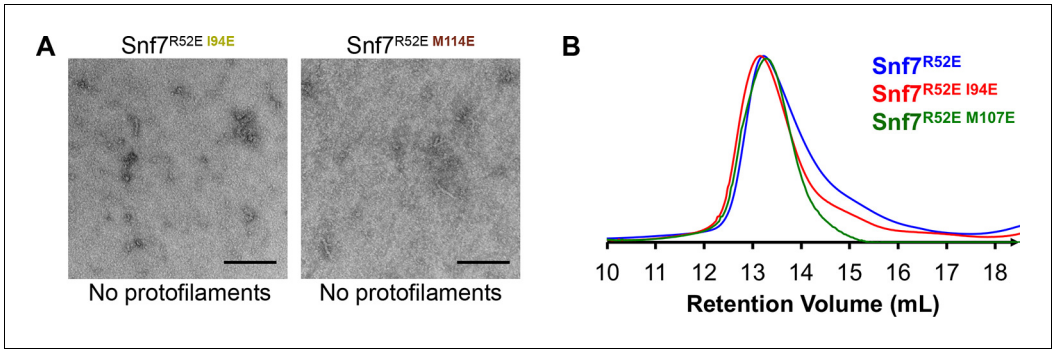

Figure 4—figure supplement 1. Hydrophobic Interface Mutant Analysis. (**A**) Representative TEM images of recombinant full-length Snf7^{R52EI94E} and Snf7^{R52EM114E}. Scale bars, 200nm. (**B**) Superdex-200 gel filtration size exclusion chromatograms of Snf7^{R52E}, Snf7^{R52EI94E} and Snf7$^{R52E\ M107E}$. Related to ***Figure 4H***.

DOI: http://dx.doi.org/10.7554/eLife.12548.018

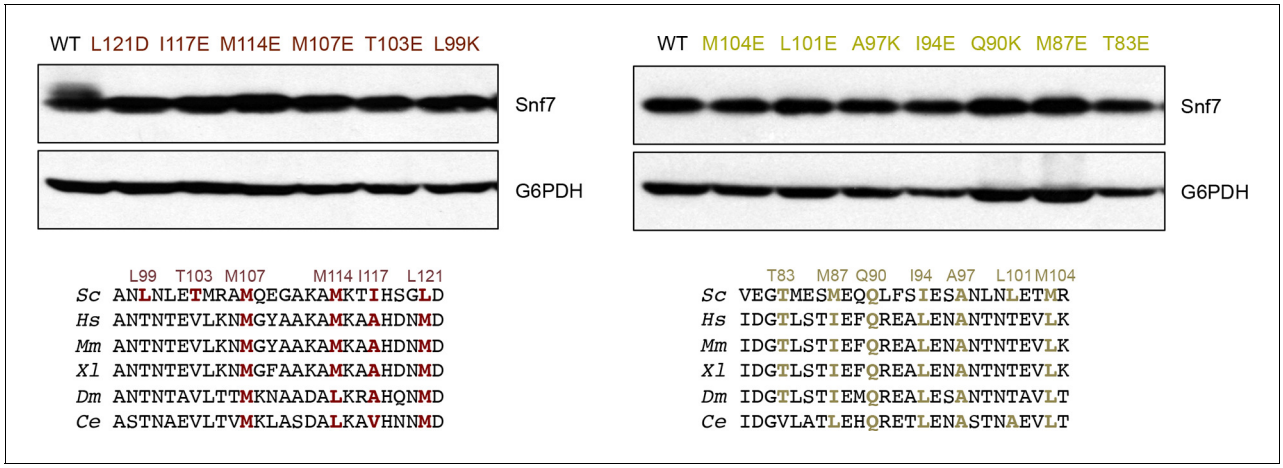

Figure 4—figure supplement 2. Western blotting analyses of *snf7*Δ yeast expressing *SNF7*, *snf7*^{L121D}, *snf7*^{I117E}, *snf7*^{M114E}, *snf7*^{M107E}, *snf7*^{T103E}, and *snf7*^{L99K}, and *SNF7*, *snf7*^{M104E}, *snf7*^{L101E}, *snf7*^{A97K}, *snf7*^{I94E}, *snf7*^{Q90K}, *snf7*^{M87E}, and *snf7*^{T83E}. G6PDH used as loading controls.

Sequence analyses of Snf7 α2/3 with conserved residues shown in gold and dark red.

DOI: http://dx.doi.org/10.7554/eLife.12548.019

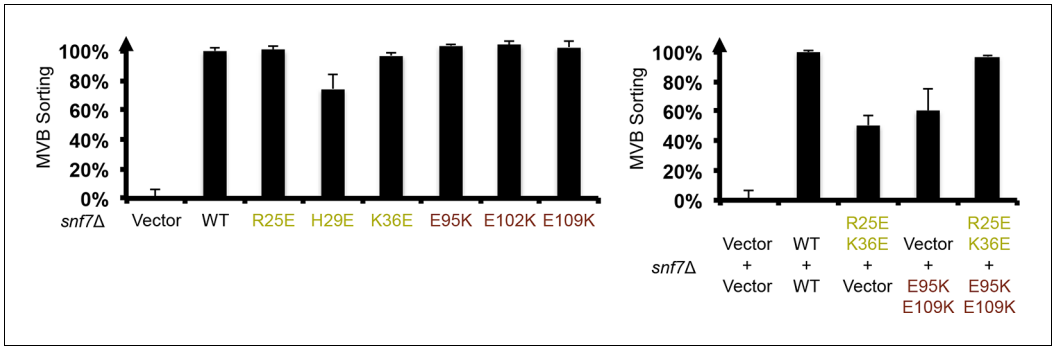

Figure 4—figure supplement 3. Quantitative MVB sorting data for *snf7Δ* yeast exogenously expressing empty vector, *SNF7*, $snf7^{R25E}$, $snf7^{H29E}$, $snf7^{K36E}$, $snf7^{E95K}$, $snf7^{E102K}$, *and* $snf7^{E109K}$, and empty vector, *SNF7*, $snf7^{R25E\ K36E}$and *vector*, *vector* and $snf7^{E95K\ E109K}$, $snf7^{R25E\ K36E}$and $snf7^{E95K\ E109K}$. Error bars represent standard deviations.
DOI: http://dx.doi.org/10.7554/eLife.12548.020

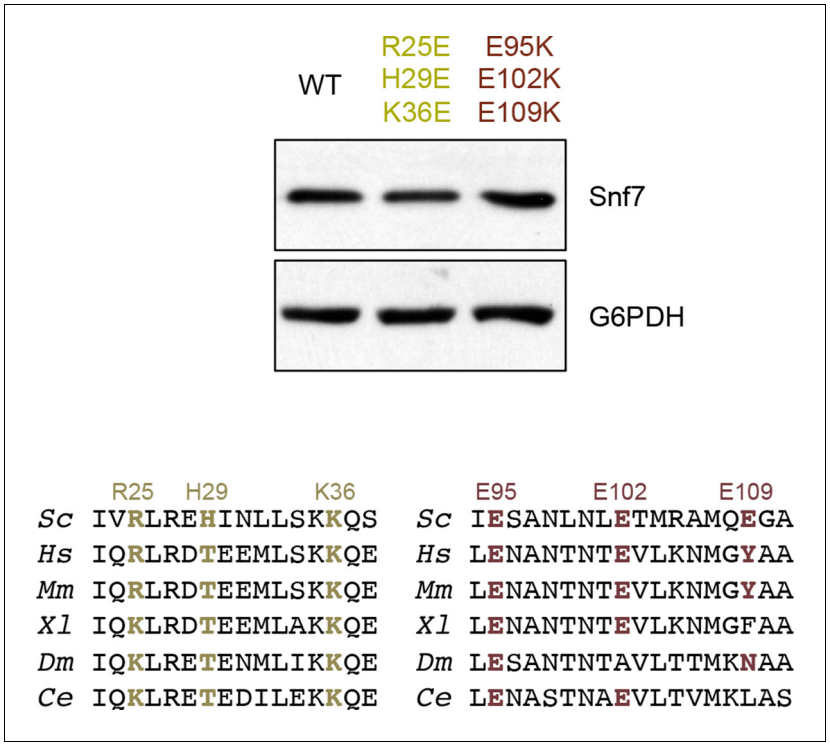

Figure 4—figure supplement 4. Western blotting analyses of *snf7*Δ yeast expressing *SNF7*, *snf7*$^{R25E\ H29E\ K36E}$, and *snf7*$^{E95K\ E102K\ E109K}$. Sequence analyses of Snf7 α2/3 with conserved residues shown in gold and dark red.

DOI: http://dx.doi.org/10.7554/eLife.12548.021

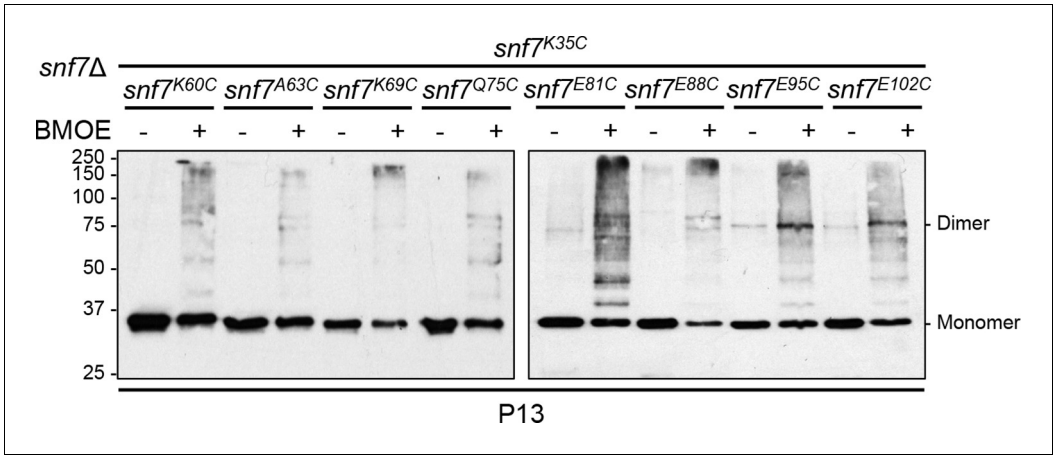

Figure 4—figure supplement 5. Western blotting analyses of *ex vivo* P13 fractions BMOE crosslinking by Snf7^{K35C} with Snf7^{K60C}, Snf7^{A63C}, Snf7^{K69C}, Snf7^{Q75C}, Snf7^{E81C}, Snf7^{E88C}, Snf7^{E95C}, and Snf7^{E102C}.

DOI: http://dx.doi.org/10.7554/eLife.12548.022

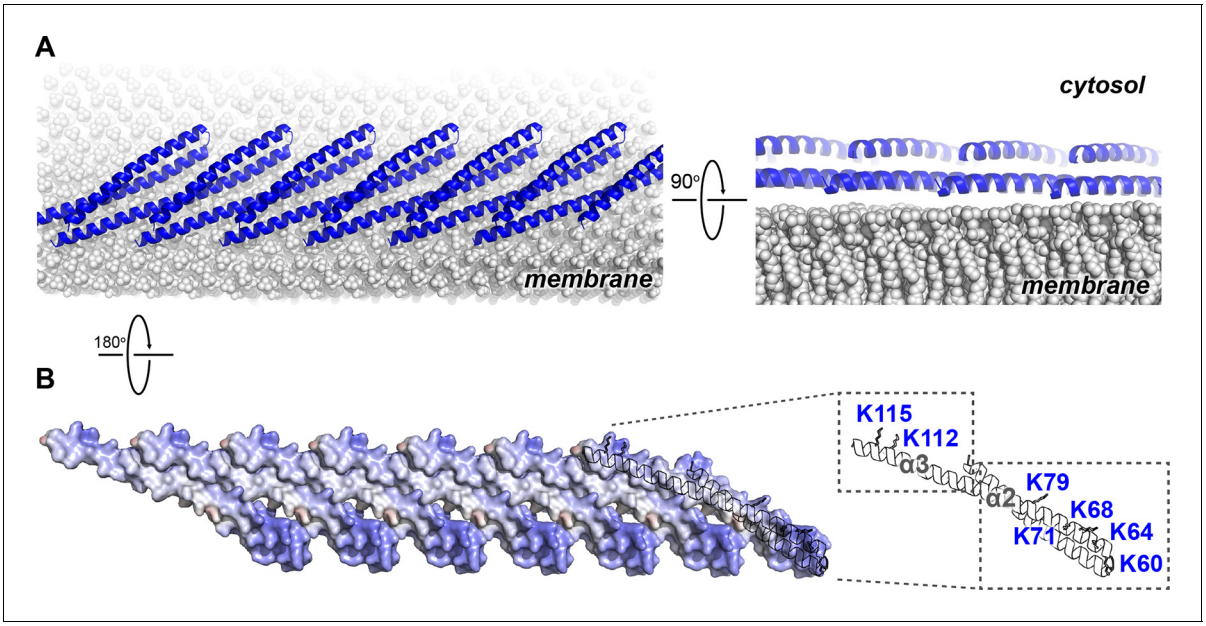

Figure 5. Electrostatic Protein-membrane Interactions in a Snf7 Filament (**A**) A Snf7 protofilament in ribbons placed on a lipid membrane in spheres (grey) (***Heller et al., 1993***). (**B**) Electrostatic surface potential showing the membrane interacting surface of a Snf7protofilament with positively charged regions in blue (+10kcal/e$^-$) and negatively charged regions in red (-10kcal/e$^-$).

DOI: http://dx.doi.org/10.7554/eLife.12548.023

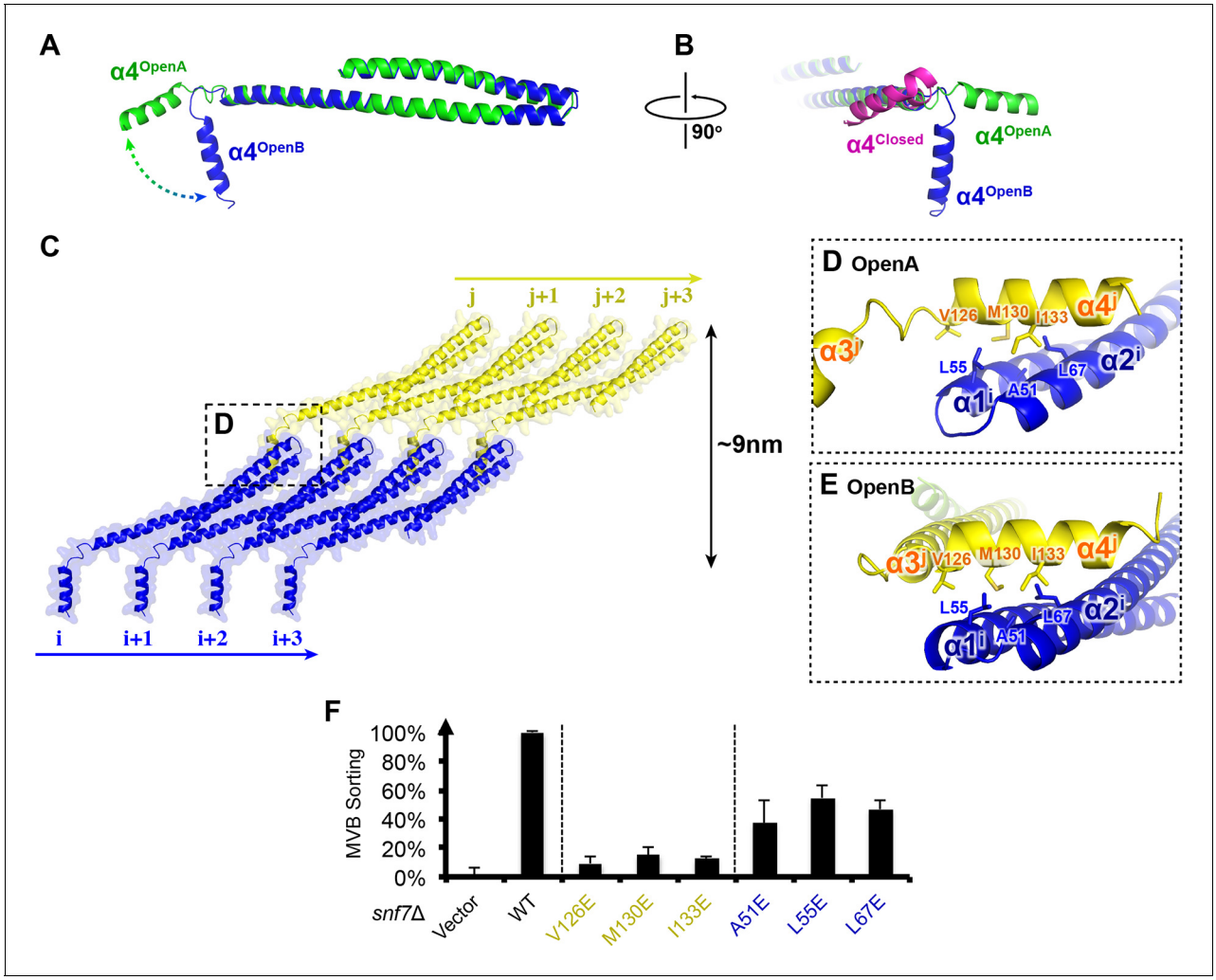

Figure 6. Snf7 α4 in Inter-Filament Interactions (**A–B**) Snf7^{core} conformations A (green) and B (blue) superimposed. (**B**) 90° rotation and superimposing with a closed CHMP3 (purple) using its α3 as a reference. (**C**) Overlay of ribbon and space-filling models of the Snf7^{core} crystal packing of the open conformation A. The dash-line box represents the interfilament contacts. Arrows represent inter-protofilament orientations. (**D–E**) Close-up views of the hydrophobic interface between α1/2^{i} (blue) and α4^{j} (yellow) of open conformations (**D**) A and (**E**) B. (**F**) Quantitative MVB sorting data for *snf7*Δ yeast exogenously expressing empty vector, *SNF7*, *snf7*^{V126E}, *snf7*^{M130E}, *snf7*^{I133E}, *snf7*^{A51E}, *snf7*^{L55E}, and *snf7*^{L67E}. Error bars represent standard deviations. See also ***Table 1***.

DOI: http://dx.doi.org/10.7554/eLife.12548.024

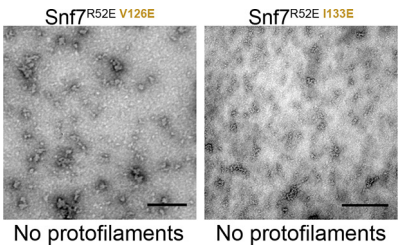

Figure 6—figure supplement 1. Representative TEM images of recombinant full-length Snf7$^{R52E\ V126E}$ and Snf7$^{R52E\ I133E}$. Scale bars, 200nm.

DOI: http://dx.doi.org/10.7554/eLife.12548.025

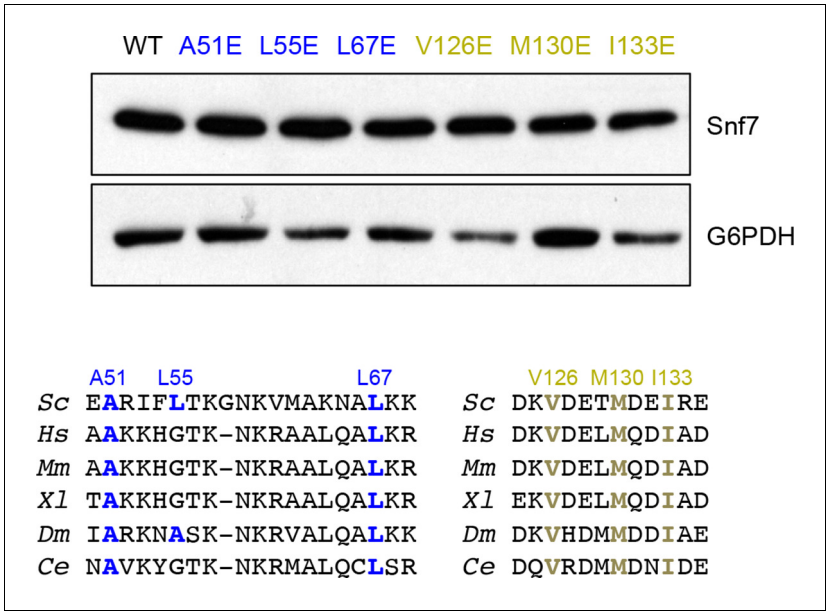

Figure 6—figure supplement 2. Western blotting analyses of *snf7*Δ yeast expressing *SNF7*, $snf7^{A51E}$, $snf7^{L55E}$, $snf7^{L67E}$, $snf7^{V126E}$, $snf7^{M130E}$, and $snf7^{I133E}$. G6PDH as a loading control.

Sequence analyses of Snf7 α1/2 and α4 with conserved residues shown in blue or gold.

DOI: http://dx.doi.org/10.7554/eLife.12548.026

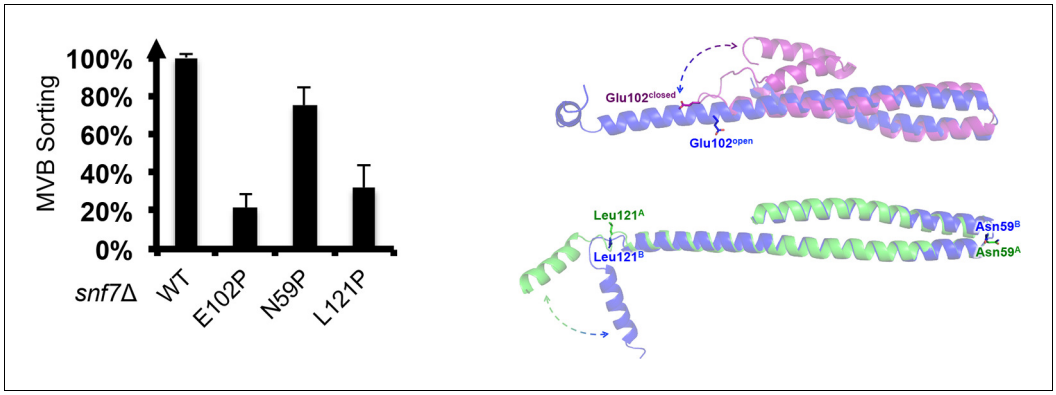

Figure 6—figure supplement 3. Quantitative MVB sorting data for *snf7Δ* yeast exogenously expressing *SNF7*, $snf7^{E102P}$, $snf7^{N59P}$, and $snf7^{L121P}$. Error bars represent standard deviations. Overlay ribbon models of (upper right) closed (purple) and open (blue) $Snf7^{core}$ with Glu102 shown in sticks, and (lower right) open conformation A (green) and B (blue) with Asn59 and Leu121 shown in sticks. Arrows represent conformational rearrangements.
DOI: http://dx.doi.org/10.7554/eLife.12548.027

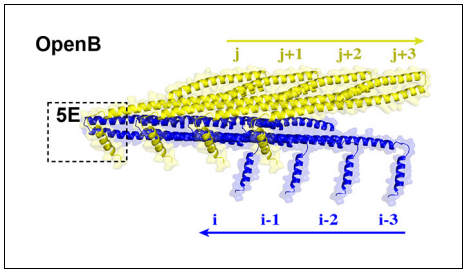

Figure 6—figure supplement 4. An overlay of ribbon and space-filling models of the Snf7^{core} crystal packing of the open conformation B. The dash-line box represent the interfilament contacts shown in ***Figure 6E***.

DOI: http://dx.doi.org/10.7554/eLife.12548.028

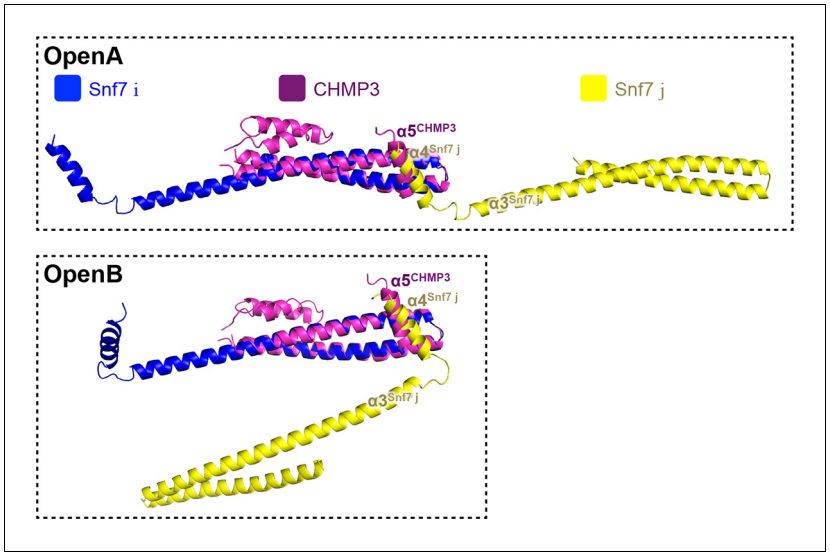

Figure 6—figure supplement 5. Superimposing of Snf7^{core} subunit (i) (blue), (j) (yellow) and CHMP3$^{\alpha 1\text{-}\alpha 5}$ (purple) of open conformations A (upper) and B (lower).
DOI: http://dx.doi.org/10.7554/eLife.12548.029

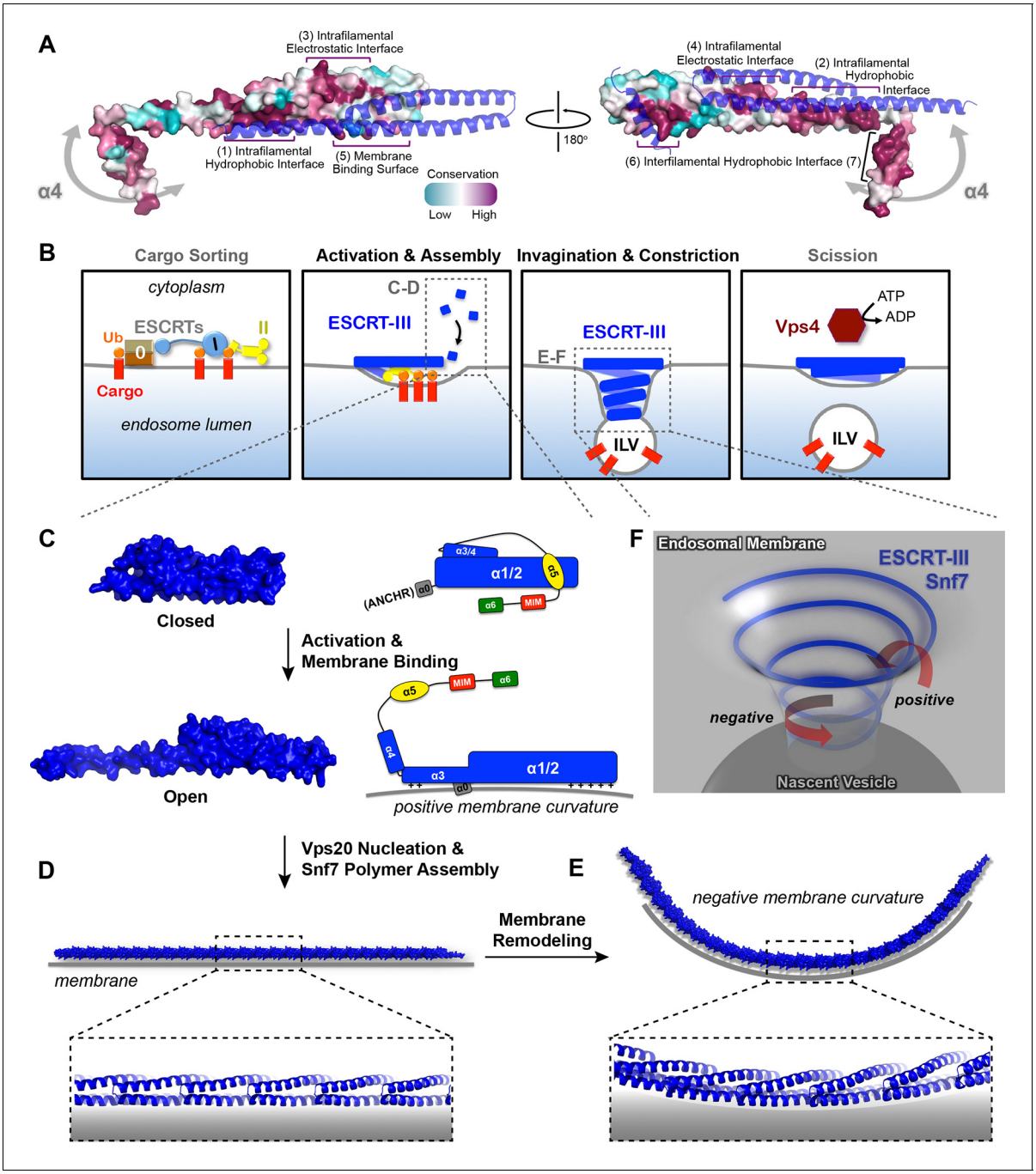

Figure 7. Models of Snf7 activation, polymer assembly and membrane remodeling (**A**) Space-filling CONSURF models with high conservation (purple) and low conservation (cyan). Interacting protomers shown in ribbon (blue). Seven conserved regions with assigned functions labeled. Gray arrows indicate the flexibility of α4. (**B**) Speculative cartoons illustrating four stages in ESCRT-mediated vesicle budding. (**C**) Space-filling models and schematic cartoons of $Snf7^{core}$ in closed and open states with membrane (grey). (**D**) Space-filling and close-up ribbon models of a 25-mer Snf7 single filament with membrane. (**E**) Space-filling and close-up ribbon models of a 23-mer Snf7 normal mode analysis filament with membrane (grey). (**F**) Schematic of a Snf7 homo-polymer in the neck of a nascent ILV with positive and negative membrane curvatures.

DOI: http://dx.doi.org/10.7554/eLife.12548.030

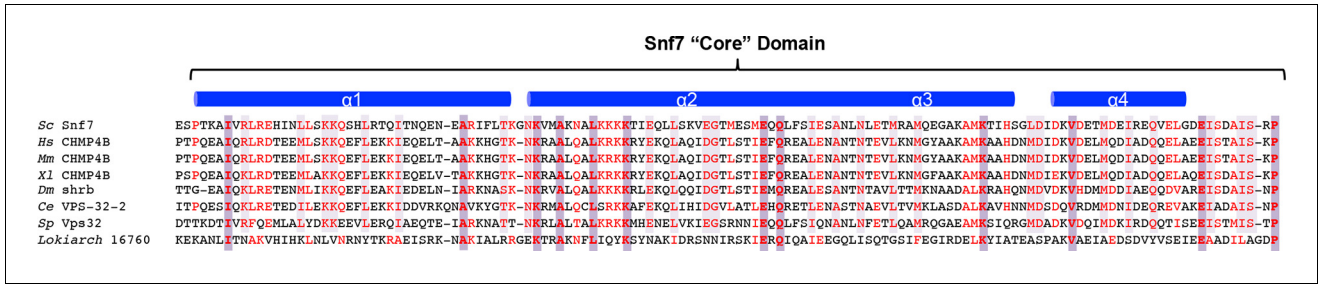

Figure 7—figure supplement 1. Alignment of Snf7^{core} protein sequences from *Saccharomyces cerevisiae (Sc), Homo sapiens (Hs), Mus musculus (Mm), Xenopus laevis (Xl), Drosophila melanogaster (Dm), Caenorhabditis elegans (Ce), Schizosaccharomyces pombe (Sp)* and *Lokiarchea* (***Spang et al., 2015***).
DOI: http://dx.doi.org/10.7554/eLife.12548.031

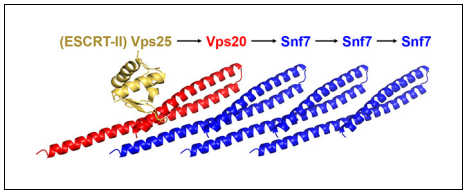

Figure 7—figure supplement 2. A ribbon model of a supercomplex of Vps25-Vps20-Snf7. The first Snf7's α1 was used for superimposing with the Vps20 α1 (***Im et al., 2009***) (PDB: 3HTU) for molecular docking.
DOI: http://dx.doi.org/10.7554/eLife.12548.032

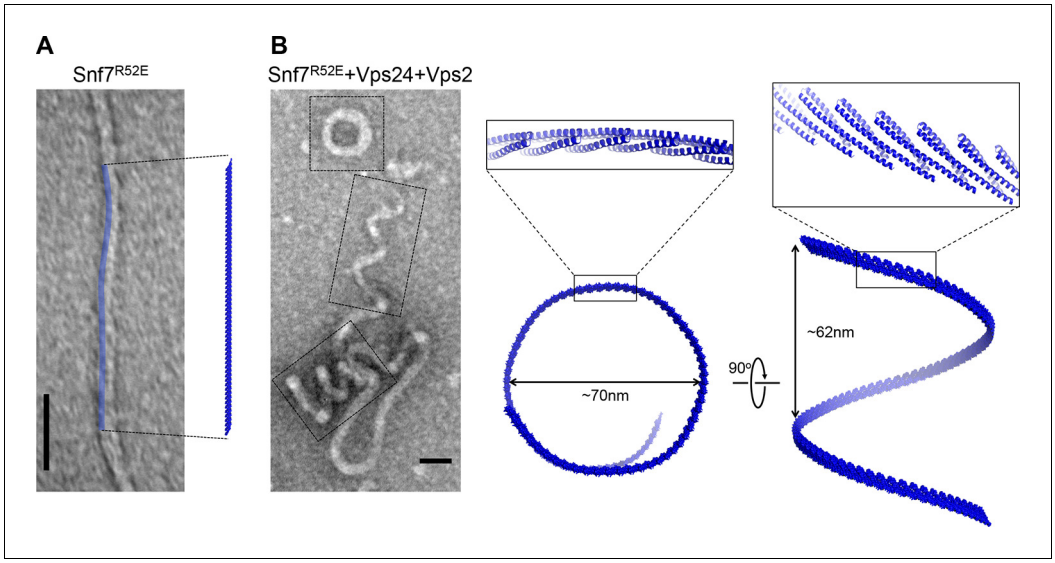

Figure 7—figure supplement 3. Architectures of Snf7 protofilaments (**A**) A representative TEM image of recombinant Snf7^{R52E} (left) and a space-filling model of a 61-mer Snf7$^{\alpha 1\text{-}3}$ straight filament shown in the same scale (right). (**B**) A representative TEM image of recombinant full-length Snf7^{R52E}, Vps24 and Vps2 (2:1:1) (left), and space-filling and close-up view of ribbon models of a 97-mer Snf7$^{\alpha 1\text{-}3}$ superhelix generated by normal mode analysis with measured dimensions (right). TEM scale bars, 50nm.

DOI: http://dx.doi.org/10.7554/eLife.12548.033